JOURNAL OF CATALYSIS **176,** 527–535 (1998)
ARTICLE NO. CA982076

AMM-Mn_xSi-Catalyzed Selective Oxidation of Toluene

Frank Konietzni,* Uwe Kolb,* Uwe Dingerdissen,† and Wilhelm F. Maier*,[1]

*Max-Planck-Institut für Kohlenforschung, Kaiser-Wilhelm-Platz 1, D-45470 Mülheim an der Ruhr, Germany; and †Hoechst AG, D-65926 Frankfurt am Main, Germany

Received November 25, 1997; revised March 9, 1998; accepted March 9, 1998

Amorphous, microporous mixed oxides, based on silica with isolated Mn centers in the amorphous silica matrix, were prepared by means of an acid catalyzed sol–gel process. The materials have a narrow micropore distribution with a pore diameter of 0.8 nm. XANES investigations of the materials on the Mn absorption edge provide evidence that isolated octahedrally coordinated Mn^{II} sites predominate. Further characterizations include XRD, sorption measurements, and light microscopy. The good activity of the new catalysts for the selective oxidation of toluene to benzaldehyde is attributed to the homogeneously distributed manganese in the shape selective environment of the micropores. © 1998 Academic Press

INTRODUCTION

The selective direct oxidation of hydrocarbons with air to oxygenated products such as alcohols, aldehydes, and ketones is technically of high interest. The increased reactivity of the products relative to the starting materials makes selective oxidation difficult, because secondary reactions are faster. The well-known kinetic consequences of such *successive* reactions (1) often require low conversion, short residence time, and reaction control (no transport limitation) to achieve acceptable selectivities. These requirements usually result in undesirable conditions for chemical production, leading to inefficient use of energy, high process costs, and chemical waste. Natural catalysts, such as enzymes, overcome these problems in an elegant way by inhibiting secondary reactions of the product through a reaction selectivity based on chemical recognition. In technical catalysts catalytically active centers, capable of selective oxidation and better control of access of reagents to these centers, are required. Such catalysts have not been obtained by conventional routes and new materials are required to achieve the desired higher selectivities.

Due to the facile control of catalyst characteristics such as elemental compositions, surface areas, pore size distributions, and surface polarity in a single step preparation process, we successfully used sol–gel procedures to prepare defined catalysts for heterogeneously catalyzed reactions such as selective oxidation with organic hydroperoxides (2, 3) or H_2O_2 (4) or shape selective hydrocracking (5). The acid catalyzed sol–gel process, initiated by linear chain growth, leads to amorphous, microporous oxides (AMM) with a narrow pore size distribution and large surface areas (6). The incorporation of active metals into a microporous matrix provides materials with a wide range of potential applications.

We here report our studies of the formation of benzaldehyde by selective air oxidation of toluene with an amorphous, microporous Mn/Si mixed oxide. Benzaldehyde is still produced by the hydrolysis of benzal chloride, obtained by side chain chlorination of toluene. Although there are several catalysts, most of which are based on molybdenum, that can be used for the gas phase oxidation of toluene to benzaldehyde, this direct oxidation is rarely used in industry. A major source of benzaldehyde is its formation as a side product in the Dow process.

Although the oxidation of toluene can be achieved without catalysts, the product is composed of about equal amounts of benzaldehyde, benzylalcohol, and benzoic acid, even at a low conversion of 6% (7). K_2FeO_4 has been reported for selective oxidation reactions in the liquid phase at low temperatures (8). A disadvantage is the rather low activity for toluene oxidation and the formation of $Fe(OH)_3$ during the reaction. Gas phase oxidation of toluene has attracted more interest than liquid phase conditions (9). Many of the catalysts described are based on molybdenum in combination with tungsten (10), manganese (11), cerium (12), or iron (13) in the form of mixed oxides or based on carriers such as molecular sieves (14, 15). One of the most promising gas phase catalysts for benzaldehyde production, free of molybdenum, is based on V_2O_5-supported on TiO_2, SiO_2, or Al_2O_3 (16–19). The catalytic activity of these catalysts could be increased in some cases with additives such as K_2SO_4 (19).

Nearly all of the catalysts mentioned above were prepared by wet impregnation. While this method is relatively inexpensive and easy to carry out, it leads to a small number of active sites, domain formation, and drastically decreases

[1] Author to whom correspondence should be addressed.

0021-9517/98 $25.00
Copyright © 1998 by Academic Press
All rights of reproduction in any form reserved.

the surface area of the catalysts. It is preferable to have catalysts with a high concentration of active (isolated) sites on a large surface area; this can be achieved by the sol–gel method.

EXPERIMENTAL

Catalyst Preparation

The chemical composition of the sol for the preparation of the AMM-Mn_xSi catalysts is given by

$$Mn^{III}\text{-acetate } 2\,H_2O : TEOS : H_2O : HCl : EtOH = x : (100 - x) : 200 : 35 : 300,$$

where x is the relative molar amount of manganese acetate. The manganese salt was dissolved in ethanol in a polypropylene beaker. Then the TEOS (tetraethylorthosilicate) was added while stirring. The gelation process was started by adding water and hydrochloric acid in an 8N solution while stirring. The beaker was covered with parafilm. Gelation was obtained after about two to three weeks. After drying, the catalysts were calcined using the temperature program: RT $\rightarrow$ 0.2 K/min $\rightarrow$ 65°C (300 min) $\rightarrow$ 0.5 K/min $\rightarrow$ 400°C (300 min) $\rightarrow$ RT.

Physicochemical Characterization

The XANES experiment was performed at the Mn-K-edge at station BN3 of the synchrotron radiation source ELSA (University of Bonn, Germany). A double crystal monochromator, equipped with two Ge [220] crystals, was used and calibrated with a manganese foil (6540.0 eV). The experiment was conducted in the transmission mode with a standard experimental set-up. The sample was prepared by mixing the powder with polyethylene und pressing pellets of 13-mm diameter. The homogeneity of the sample was controlled optically.

The photographs were taken with a Nikon Optiphot-2 light microscope.

Ar adsorption isotherms were obtained at liquid argon temperature with an Omnisorp 360 using the continuous flow technique for adsorption and desorption. Samples were heated to 250°C and evacuated for 12 h at a pressure of 1×10^{-6} Torr. The micropore distribution was calculated by the Horvath–Kawazoe method (20). X-ray powder diffraction patterns (XRD) were measured with a Stadi2/PL diffractometer. The XRD patterns were obtained with a Stoe Stade 2/PL powder diffraction system.

The AMM materials were examined with high resolution transmission electron microscopy (HRTEM) on a HITACHI HF 2000 instrument combined with energy dispersive X-ray analysis (EDX). Elemental distribution was investigated by selected area EDX microanalyses with area sizes varying from 2 nm to several μm. The samples were crushed in an agate mortar in a methanol suspension and transferred to a holey carbon grid (copper, 3-mm diameter).

Catalytic Oxidation of Toluene

The catalytic activity of the prepared AMM-MnSi catalysts in the selective oxidation of toluene to benzaldehyde was tested under gas phase flow conditions in a tubular fixed-bed reactor. The reactor, a quartz glass tube (450-mm length, 6-mm diameter), is surrounded by an electrical heater. The air flow at the inlet of the reactor is controlled by a mass flow controller, while the toluene is added by a syringe pump. Fifty milligrams of the ground catalyst were mixed with 1 g α-Al_2O_3 (particle size $<$200 μm) to avoid pressure drops in the catalyst bed, which was fixed in the middle of the tube with quartz wool. The reaction products were collected in a cold trap (−78°C), after the reactor for GC-analysis. An IR gas sensor (Winter) at the reactor outlet was used to monitor the carbon dioxide formed during the reaction. Synthetic air and toluene, purified by distillation from a predried molecular sieve, were used as reaction components. A reaction temperature of 742 K was found to be best for the catalytic oxidation of toluene. At this temperature no autoxidation is observable in the empty tube. The catalytic oxidation by Al_2O_3 does not exceed 0.7%. The molar ratio of oxygen to toluene was 7.7 at a WHSV of 11, 6 h^{-1} (flow: 90 ml/min) for most of the reactions.

RESULTS AND DISCUSSION

Catalyst Preparation

The acid-catalyzed sol–gel process leads to a clear gel after drying. The colorless Mn^{III}-acetate solution turns brown upon the addition of hydrochloric acid. After several hours (depending on the manganese content) the sol becomes colorless again within 1 min. This gelation behavior suggests a change in the oxidation state of the manganese during the sol–gel process. The reducing agent may be the ethanol used as the solvent, leading to a manganese of lower oxidation state, probably II.

Catalyst Characterization

XANES spectroscopy. A commonly used method for interpreting the edge region of an X-ray absorption spectrum is the comparison with spectra of well-defined substances. The XANES (X-ray absorption near edge structure) features of two spectra are similar when the local environments of the samples are similar (21, 22). The XANES spectrum of the measured sample AMM-Mn_4Si was compared with spectra of different manganese oxides, manganese phosphates, and aqueous $MnCl_2$ solution (21). Characteristic features of the near edge region are marked with the characters A to D, analogous to Refs. (21, 22). Empirically, it was found that the peak, marked with character

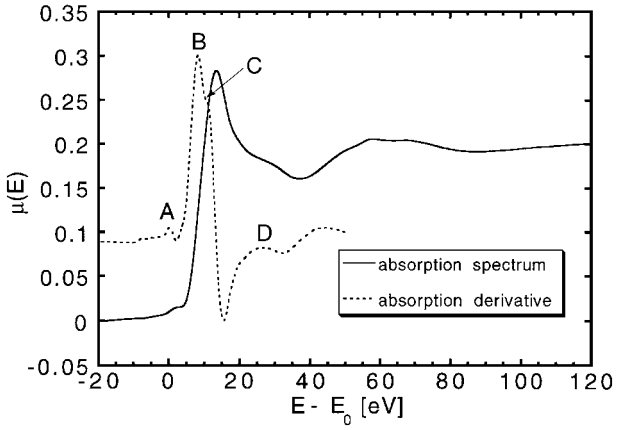

FIG. 1. Absorption spectrum (solid line) and its standardized first derivative (broken line) of the X-ray absorption coefficient of AMM-Mn_4Si vs the photon energy difference $E-E_0$. E_0 is the zero of the photoelectron energy scale, taken at the first maximum of the derivative spectrum of manganese.

A, is much stronger when the environment of the manganese atoms is tetrahedral rather than octahedral. Therefore, it can be used to determine the symmetry of the local environment around the absorber atom.

Figure 1 shows the XANES spectrum of AMM-Mn_4Si and its first derivative. Compared with the derivated spectra of (21), it resembles the spectra of Mn-ATP and of the aqueous $MnCl_2$ solution, indicating an octahedral environment. The first derivative spectra of the manganese oxides are rich in characteristic features. These features are missing in the derivative spectrum of AMM-Mn_4Si. This indicates that crystalline manganese oxide particles are not present in the sample.

If the oxidation state of the manganese atoms in the sample is determined as described in (21), then a valency around II is deduced. This does not exclude the simultaneous existence of both Mn^{2+} and Mn^{3+} in the sample. The assignment of the characteristic feature A (0.27 eV behind the edge) to an oxidation state leads to a value of 1.8, for B (8.33 eV behind the edge) to a value of 2.5 (in agreement with results published in Ref. (23)), and for C (13.4 eV behind the edge) to a value of 1.7. This method works very well for identical environments (23), but fails if the symmetry of the atoms around the absorber changes.

XRD. Figure 2 shows the XRD spectra of the sample AMM-Mn_4Si. The sample is X-ray amorphous. The spectra of the catalyst after the reaction shows several signals (Fig. 3) which correspond to the Al_2O_3 used for dilution in the catalyst bed during the reaction. No other signal appeared, indicating that the catalyst remains amorphous during the reaction.

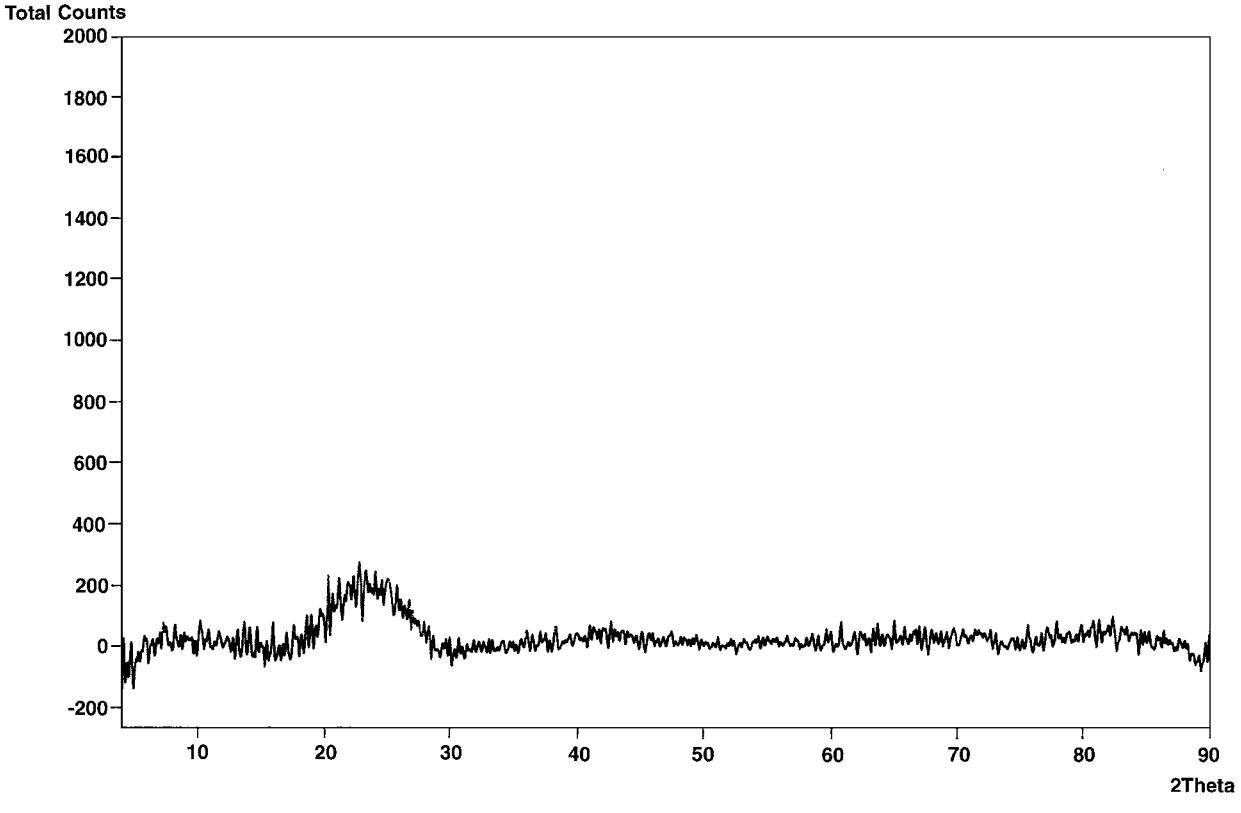

FIG. 2. X-ray diffraction pattern of AMM-Mn_4Si as prepared before catalysis.

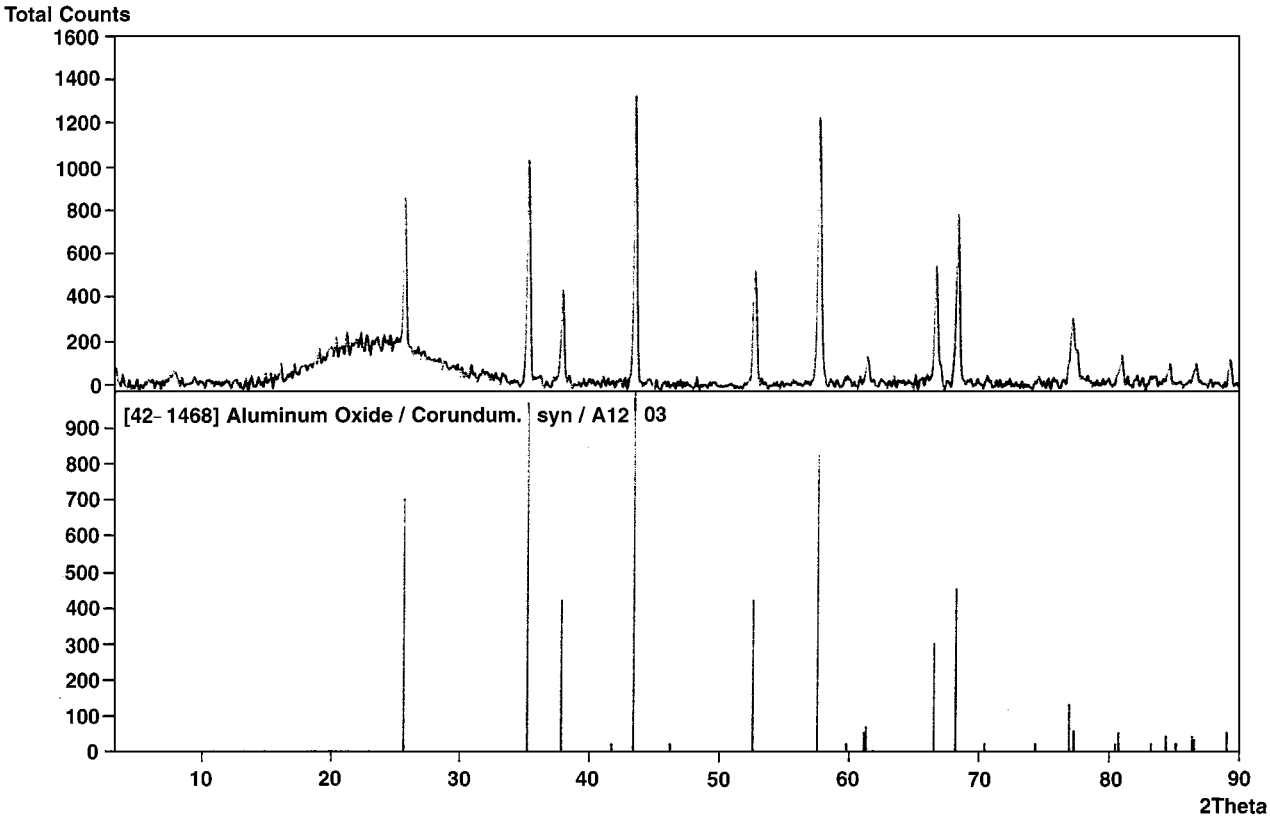

FIG. 3. X-ray diffraction pattern of AMM-Mn_4Si after catalysis and the literature XRD of Al_2O_3 indicating the presence of crystalline Al_2O_3 particles.

HR TEM/EDX. The high resolution imaging of the mixed oxides (HRTEM) confirmed the amorphous character of the materials. Neither electron diffraction patterns, typical of crystalline samples, nor crystalline lattice fringes were detected in the AMM-Mn_xSi materials. Furthermore, the homogeneous distribution of the elements was confirmed by the combination of high resolution imaging with energy-dispersive X-ray microanalysis (EDX). The Si/Mn ratios in thin particles do not depend on the area selected for the point analysis (area range: 2 nm–several (μm), confirming the homogeneous elemental distribution in the sample. The lack of evidence of the presence of Mn domains suggests a high dispersion of the Mn sites in the silica matrix.

Sorption Measurements

The acid-catalyzed sol–gel process leads to amorphous, microporous materials with a narrow pore size distribution. Figure 4 shows the pore size distribution of the four catalysts. It is obvious that the manganese content has no influence on the maximum in the pore size distribution, but a slight broadening of the pore size distribution with increasing Mn content is evident. Since most of the pores in these materials have the identical pore diameter (as shown in Fig. 4) the arithmetic mean diameter is given in Table 1, which shifts toward larger average diameters because of the increasing broadening in the pore size distribution. The BET surface areas of all samples, listed in Table 1, are high.

In conjunction with the XANES and TEM data these studies document that the materials used contain atomically isolated Mn sites in a shape selective environment (micropores).

Toluene Oxidation

To avoid the measured conversions and selectivities being controlled by mass transport to the catalyst surface or by pore diffusion phenomena, reaction controlled conditions were determined.

TABLE 1

Sample	Surface area [m^2/g]	Mean pore diameter [nm]
AMM-$Mn_{0.5}Si$	366.2	0.87
AMM-Mn_1Si	423.7	0.85
AMM-Mn_2Si	489.3	0.91
AMM-Mn_4Si	455.9	1.08

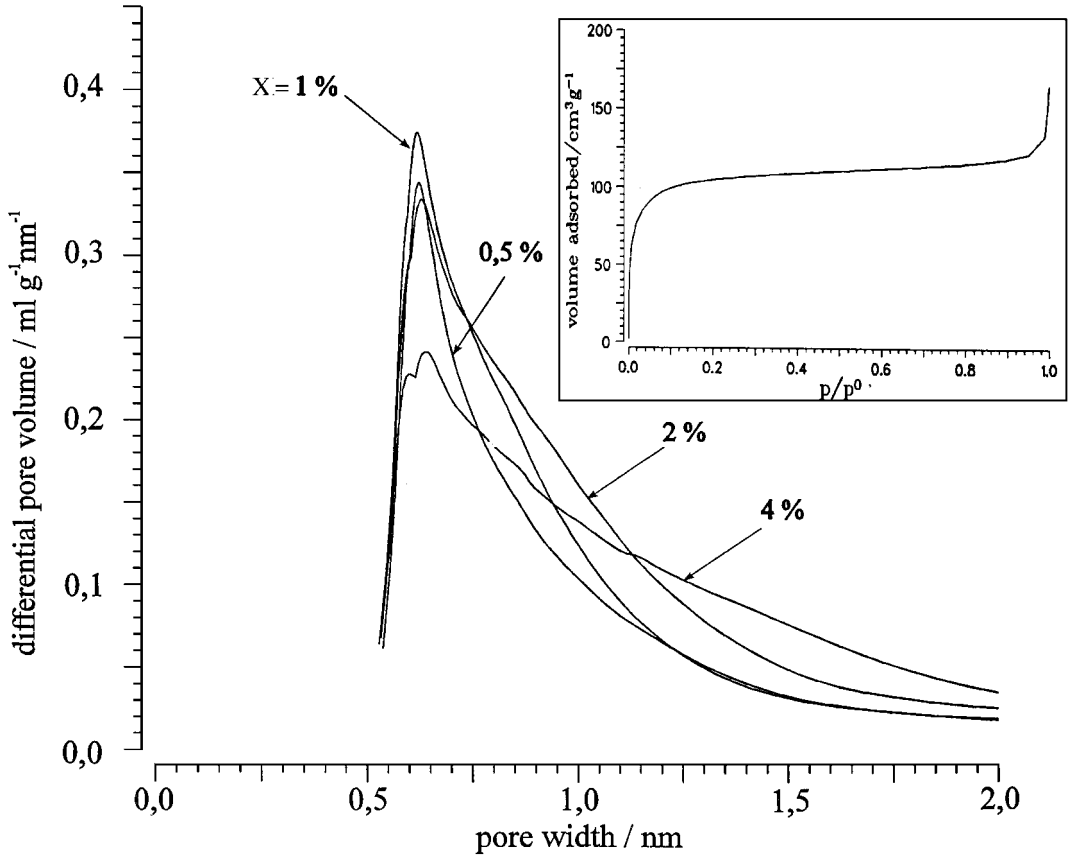

FIG. 4. Micropore size distribution of several AMM-Mn_xSi catalysts and the Ar-adsorption isotherm of the AMM-Mn_1Si.

Influence of Catalyst Mass

Figure 5 summarizes the influence of the catalyst mass (AMM-Mn_4Si) on toluene conversion and benzaldehyde yield (flow rate 90 ml/min). In these experiments the formation of carbon dioxide was monitored (ranging from 0.46 to

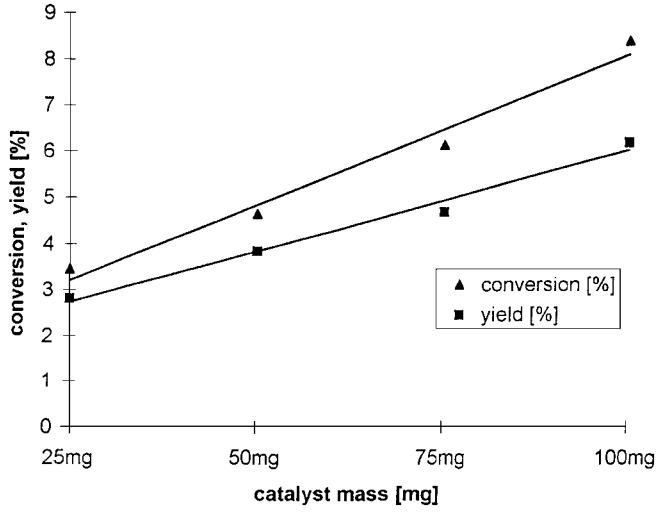

FIG. 5. Influence of catalyst mass (AMM-Mn_4Si) on toluene conversion and benzaldehyde yield.

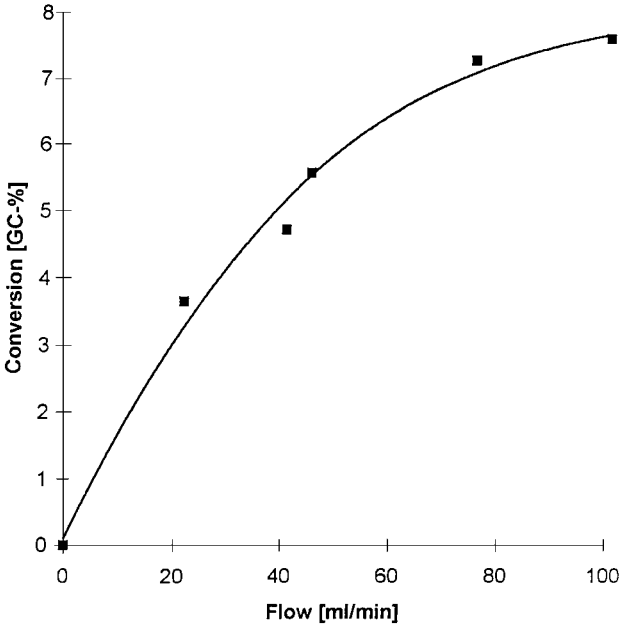

FIG. 6. Dependence of the flow rate on total toluene conversion with catalyst AMM-Mn_4Si.

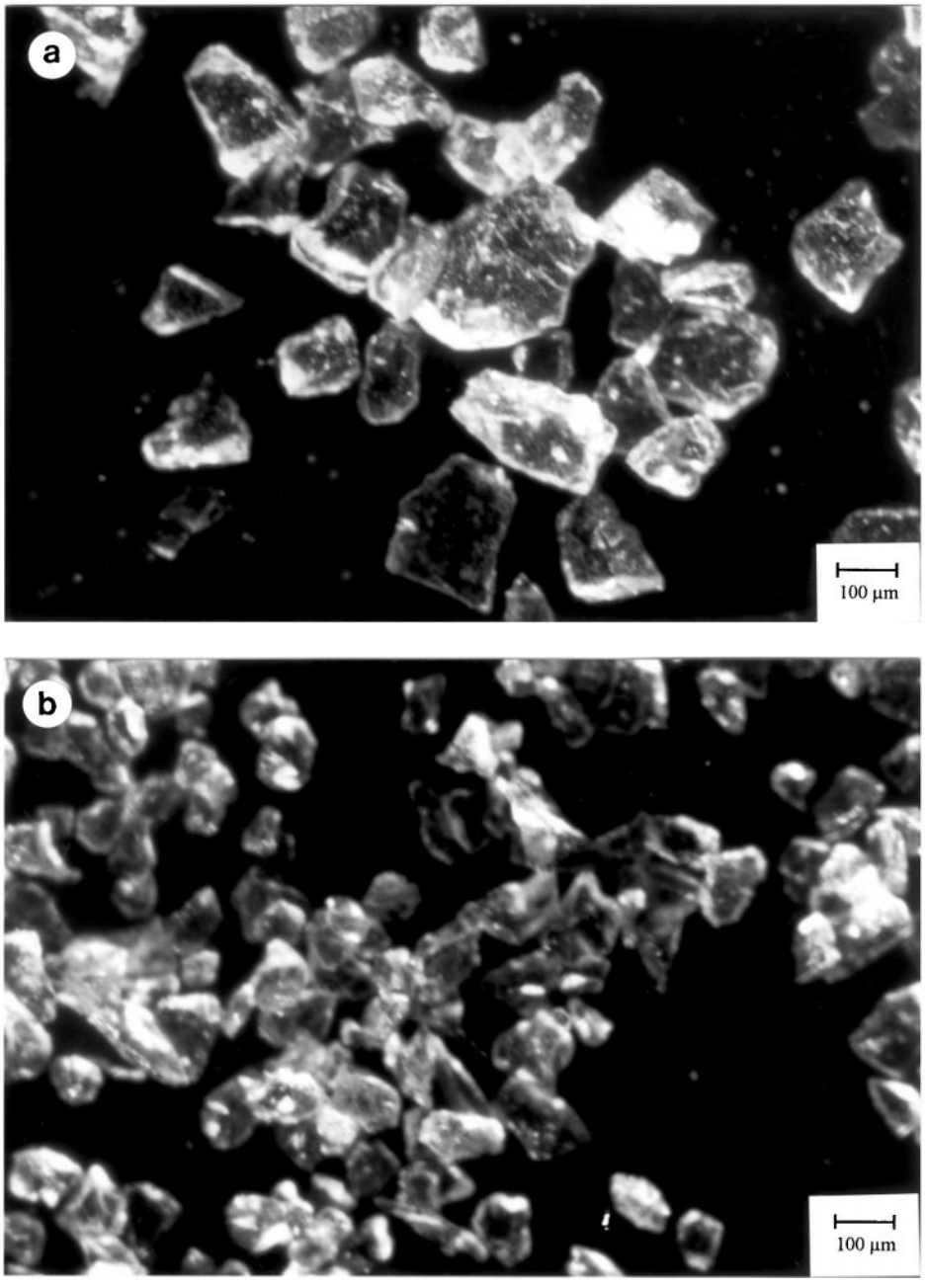

FIG. 7. Photographs at a magnification of 50 of the sieve fractions of AMM-Mn_2Si used. a, >100 μm; b, 50–100 μm; c, 20–50 μm; d, <20 μm; e, ground in a ball mill, <1–2 μm.

1.58%) and included in the toluene conversion. First-order dependence of conversion and yield on catalyst mass was obtained. As expected, the selectivity to benzaldehyde decreases with increasing conversion. Interpolation to 0% Mn does not go through the origin because of the background activity of the alumina used as dilutent (see the experimental part). With a catalyst mass of 50 mg an acceptable selectivity (83%), at a conversion around 4%, was obtained. To avoid pressure drops, this amount of catalyst was used in the remaining experiments. The pressure drops became obvious when a catalyst mass greater than 100 mg was used.

With consecutive, step wise (10°C) increase and decrease in the reaction temperature, from 360 to 400°C and back in single experiments, a slight decrease in activity was observed. This decrease in activity was attributed to coking. By heating the catalyst in air, the initial activity was always reestablished, confirming the coking hypothesis.

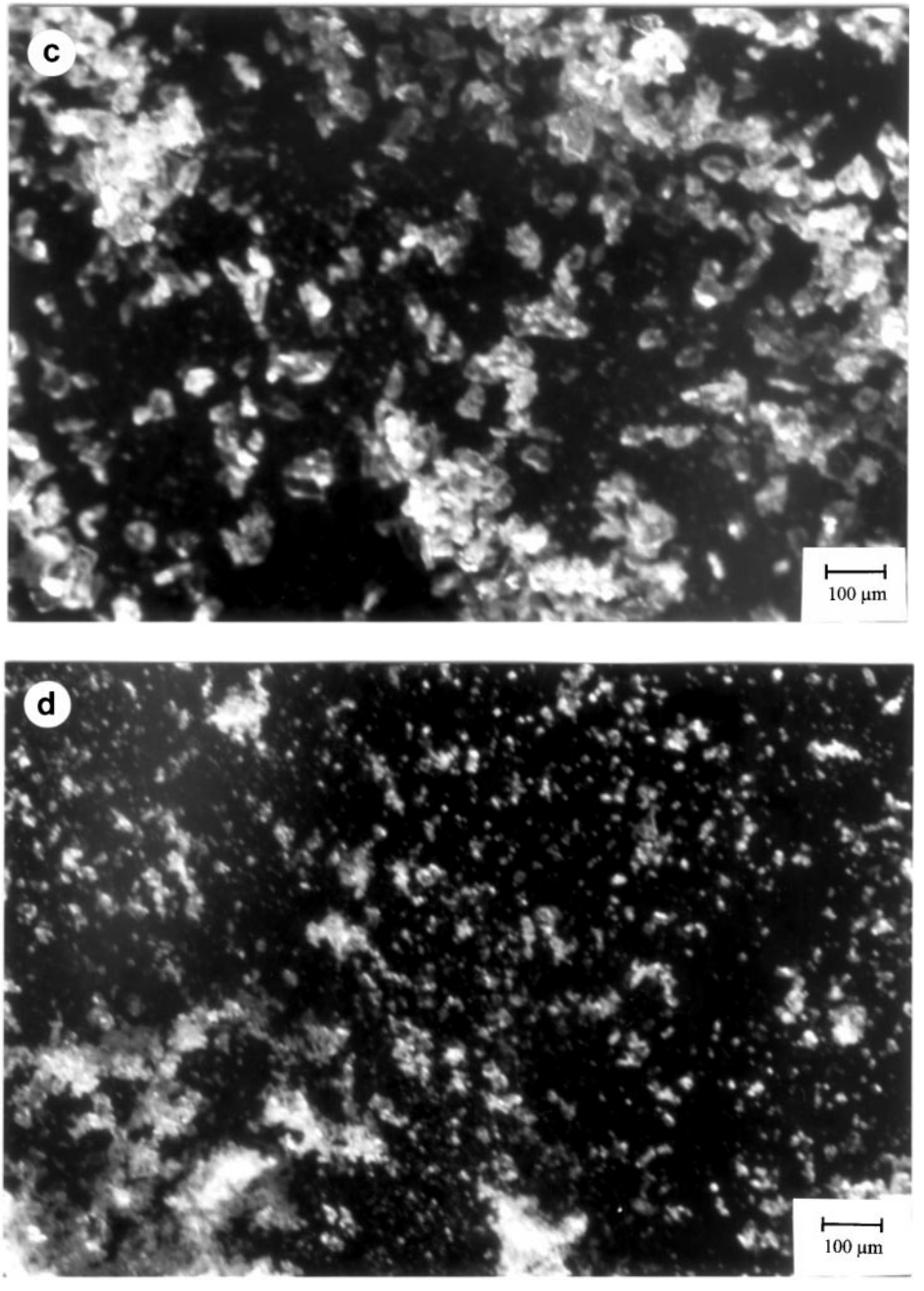

FIG. 7—*Continued*

Mass Transport Limitation

The regime of mass transport limitation was identified by varying the total flow of the reaction components through the catalyst bed while keeping the contact time constant. The catalyst mass (AMM-Mn_4Si) was increased by the same factor (25–125 mg) as the flow rate (20–100 ml) at a reaction temperature of 742 K. Figure 6 shows that, at a total flow rate above 90 ml/min, the reaction rate is not mass-transport limited.

Pore Diffusion Limitation

The influence of pore diffusion limitation on conversion was characterized by varying the particle size under constant reaction conditions (742 K, 90 ml/min total flow). The different particle sizes were separated by microsieving. Sample 1 was crushed manually in a mortar and then microsieved; sample 2 was milled in a ball mill for 30 min without further sieving. In these milled amorphous glass samples, smaller particles tend to become attached to the

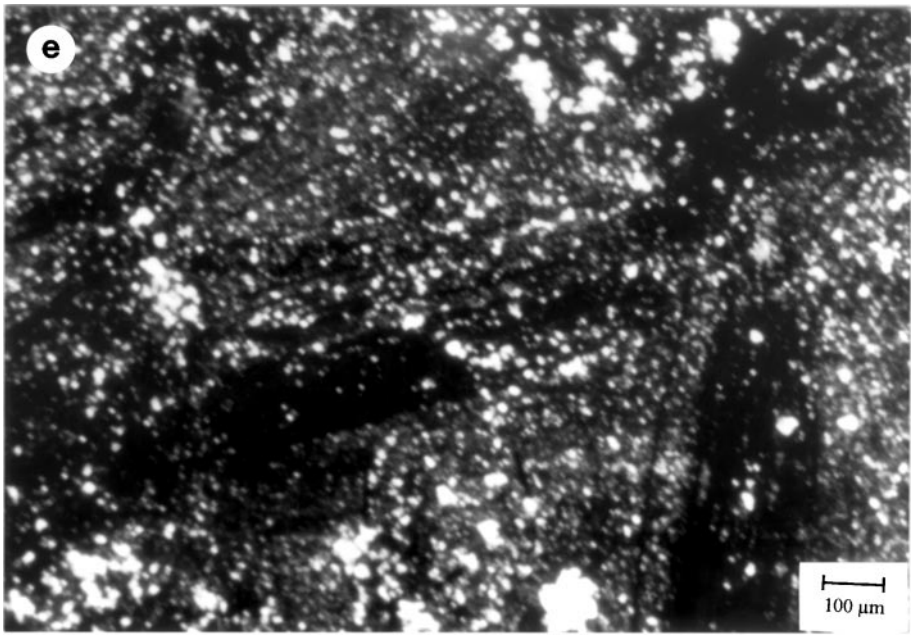

FIG. 7—*Continued*

outer surface of larger particles, thus falsifying the particle size distribution. Therefore, special care had to be taken during the sieving procedure to avoid accumulation of smaller particles in the various fractions. Figure 7 shows the different particle sizes (prepared from the same catalyst batch) used in the catalytic experiments for the catalyst AMM-Mn_2Si at a magnification of 50.

The catalytic activity was tested at 742 K (50 mg catalyst + 1 g Al_2O_3). Figure 8 shows the effect of particle size on the reaction under identical reaction conditions; this indicates a strong influence of pore diffusion limitation on conversion for bigger particles (down to 20 μm). This behavior is probably caused by the microporous character of the material (mean pore diameter around 0.8 nm). The sample which was milled in a ball mill showed the highest conversion because of the rather short diffusion length in the particles. Figure 8 shows that all larger particles are limited by pore diffusion, and even the smallest particles (particle size around 1–2 μm) may not be free of diffusion limitation. Since smaller particles could not be generated reliably by the procedures available, the dependence of catalyst activity on the Mn content was examined. If there is a first order dependence on the Mn content, then pore diffusion should not limit the reaction.

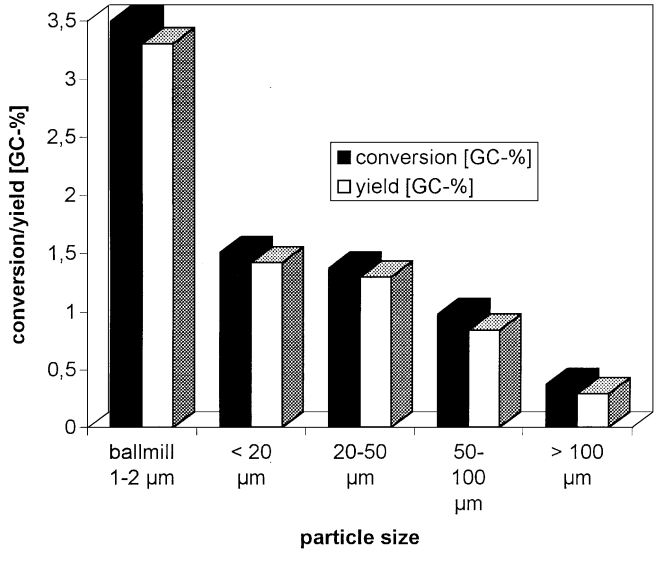

FIG. 8. Dependence of particle size on toluene conversion and benzaldehyde yield.

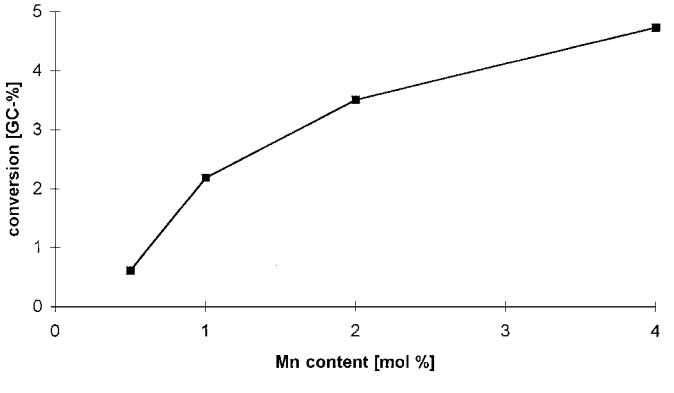

FIG. 9. Dependence of Mn content of milled AMM catalysts on total toluene conversion.

Influence of Mn Content

Figure 9 shows the increase in toluene conversion with increasing Mn content in the silica matrix at a reaction temperature of 742 K. This increase can be explained by the increase in the number of active centers in the silica matrix and shows that pore diffusion limitation probably does not occur in these small catalyst particles (1–2 μm).

Control experiments were conducted with pure MnO_2, Mn_2O_3, and MnO powders (particle size <1 μm) as catalysts. No benzaldehyde was formed at the usual reaction conditions. These results indicate that Mn oxide domains do not catalyze the selective oxidation of toluene and that the presence of isolated manganese sites in the silica lattice probably represent the active sites necessary for the selective formation of benzaldehyde from toluene.

CONCLUSIONS

Amorphous, microporous silicas with isolated Mn centers as active sites are selective catalysts for the oxidation of hydrocarbons with air as shown by the conversion of toluene to benzaldehyde. The catalysts were prepared in one step by the sol–gel process. The amorphous character of the materials was identified by XRD and TEM. XANES showed that crystalline Mn oxide domains are absent. The large surface areas of the catalysts and the isomorphic substitution of silica by manganese in the amorphous lattice lead to a high concentration of isolated, octahedrally coordinated manganese sites. Control experiments using pure MnO_2 and MnO showed poor selectivity, indicating that isolated Mn sites are necessary for selective oxidation reactions. A change in the oxidation state during the sol–gel process, from three to two, seems to increase the oxidation potential of the manganese. After determining reaction conditions that exclude mass transport and pore diffusion limitations, selectivities of 83% were achieved at a total conversion of 4%.

ACKNOWLEDGMENTS

We thank S. Storck for TEM measurements, S. Neunerdt, and H. Orzesek for preliminary experiments and the HOECHST AG for financial support.

REFERENCES

1. Wheeler, A., "Advances in Catalysis Vol. III" (W. G. Frankenburg, V. I. Komarewsky, and E. K. Rideal, Eds.), p. 252. Academic Press Inc., New York, 1951.
2. Klein, S., Thorimbert, S., and Maier, W. F., *J. Catal.* **163**, 477 (1996).
3. Klein, S., Martens, J., Parton, R., Vercruysse, K., Jacobs, P. A., and Maier, W. F., *Catal. Lett.* **38**, 209 (1996).
4. Klein, S., and Maier, W. F., *Angew. Chem.* **108**, 2376 (1996). [*Int. Ed.* **35**, 2330 (1996)]
5. Maier, W. F., Klein, S., Martens, J., Heilmann, J., Parton, R., Vercruysse, K., and Jacobs, P. A., *Angew. Chem.* **108**, 222 (1996). [*Int. Ed.* **35**, 180 (1996)]
6. Tilgner, I.-C., Fischer, P., Bohnen, F. M., Rehage, H., and Maier, W. F., *Microp. Mat.* **5**, 77 (1995).
7. Henryk, A., U.S. Patent 3,714,263.
8. Delaude, L., and Laszlo, P., *J. Org. Chem.* **61**, 6360 (1996).
9. Costantini, M., and Krumenacker, L., *Stud. Surf. Sci. Catal.* **44**, 159 (1989).
10. Reddy, K. A., and Doraiswamy, L. K., *Chem. Eng. Sci.* **24**, 1415 (1969).
11. Barbaux, Y., Dejonghe, S., Gengenbre, L., and Grzybowska, B., *React. Kinet. Catal. Lett.* **47**, 1 (1992).
12. Fan, Y., Kuang, W., and Chen, Y., *Chem. Let.* **3**, 231 (1997).
13. Zhang, H., Shen, J., and Ge, X., *Hyperfine Interact.* **69**, 859 (1991).
14. Yoo, J. S., Lin, P. S., and Elfline, S. D., *Appl. Catal. A General* **124**, 139 (1995).
15. Yoo, J. S., *Appl. Catal. A General* **143**, 29 (1996).
16. Matralis, H. K., Papadopoulou, C., Kordulis, C., Elguezabal, A. A., and Corberan, V. C., *Appl. Catal. A General* **126**, 365 (1995).
17. Elguezabal, A. A., and Corberan, V. C., *Catal. Today* **32**, 265 (1996).
18. Gündüz, G., and Akpolat, O., *Ind. Eng. Chem. Res.* **29**, 45 (1990).
19. Das, A., Chatterji, S. K., and Ray, S. K., *Fuel Sci. Technol.* **10**, 85 (1991).
20. Horvath, G., and Kawazoe, K., *J. Chem. Eng. Jpn* **16**, 470 (1983).
21. Belli, M., Scafati, A., Bianconi, A., Mobilio, S., Pallandino, L., Reale, A., and Burattini, E., *Solid State Comm.* **35**, 355 (1980).
22. Grunes, L. A., *Phys. Rev. B* **27**, 2111 (1983).
23. Bossek, U., Hummel, H., Weyhermüller, T., Wieghardt, K., Russel, S., van der Wolf, L., and Kolb, U., *Angew. Chem.* **108**, 1653 (1996).